

UNIOSUN Journal of Engineering and Environmental Sciences. Vol. 4 No. 1. March. 2022

A Comparative Study on the Aerodynamic Characteristics of National Advisory Committee for Aeronautics (NACA) 0008 and 0020 Series

Ogunnigbo, C.O., Alamu, O.J., Ochoche, O.S. and Ojerinde, B.J.

Abstract: Energy from wind is observed to be among the most viable renewable energy sources due to its minimal cost in comparison with other sources. Hence, wind energy has an advantage over fossil-fired power plants. Airfoil aerodynamic efficiency is highly important for wind turbine aerodynamic efficiency. The study determined the aerodynamic characteristics of two symmetrical NACA 4-digit airfoils; NACA 0008 and 0020. Comparisons were made in the characteristics of the airfoils, in order to further understand and compare forces at different angle of attack. The coordinates for each airfoil were developed and simulation carried out using ANSYS CFX after generating a mesh and selecting boundary conditions. The results showed that symmetrical NACA 0008 experienced high lift at each angle of attack than NACA 0020. NACA 0020 had some fraction of lift over NACA 0008 only at 0° angle of attack. NACA 0008 appears to be the better of the two airfoils, having greater lift at each angle of attack which encourages its application in wind turbine.

Keywords: Airfoil, Lift and drag force, NACA 4-digits, Simulation, Symmetrical

.

I. Introduction

Airfoil is the geometry of a propeller's blade, wing, rotor, sail or turbine as seen in Figure 1 for aerodynamic force generation. The major aim for designing airfoils is to reduce drag coefficient and increase the coefficient of lift at exposure to a moving fluid. The blade profile is one of the most critical components of a wind turbine due to its role in converting kinetic energy to mechanical energy.

Recently, Computational fluid dynamics (CFD) has gained tremendous importance and popularity for researchers because of the possibilities in achieving more accurate and

Ogunnigbo, C.O. and Ojerinde, B.J. (Department of Mechanical Engineering, Faculty of Technology, Obafemi Awolowo University, Ile Ife, Osun State, Nigeria)

Alamu, O.J., (Department of Mechanical Engineering, Faculty of Engineering, Osun State University, Osogbo, Osun State, Nigeria)

Ochoche, O.S. (Department of Mechanical Engineering, Ramon Adedoyin College of Engineering and Technology, Oduduwa University, Ipetumodu, Osun State, Nigeria)

Corresponding author: charles olawale@yahoo.com

Phone Number: +2347063553894

Submitted: 23-12-2021 Accepted: 20-02-2022 faster results for different parameters of flow shape. CFD around the has shown importance in many business sectors, aerospace industry, automobiles, industrial and marine processes, and components where the velocity of fluid and performance are crucial. In CFD calculations, flow over airfoil geometry is easily investigated. Also, instead of the high cost of running experimental work, it provides better work time and, saves cost.

Researchers have examined NACA 4420 wind turbine airfoil geometry in recent studies [1-4]. Analyses were carried out by varying blade angle of attack with various wind speeds. Additionally, [5] examined drag and lift forces on the blade of a wind turbine for various angles of attack and low Reynolds number. NACA 0012 airfoil geometry for wind turbine was examined and investigated by [6]. [7] analyzed NACA 0012 airfoil profile of wind turbine with different angles of attack (4,6,8 and 10°), with a constant Reynolds number of 10°. [6] examined NACA 0015 by studying the effect of a different angle of attack on velocity profile, lift force, wake formation, flow

separation pressure profile and flow on wind turbine airfoil profile. NACA 0015 and NACA 4415 wind turbine airfoil profiles have been compared by some researchers, and evaluation was made on the flow separation dynamics, velocity contours, pressure, drag and lift. [8] gave a comparative study of NACA 4412 and NACA 6409 wind turbine airfoil geometry analysis was carried out to evaluate pressure distribution over the airfoils and lift and drag force. The influence of the angle of attack on the geometry was examined and observations were made on variation in different properties. performed aerodynamic analysis using turbulence models such as K-epsilon, Viscous for the simulation of S809 series airfoil and Spalart-Allmaras at different angle of attacks $(0 - 14^{\circ})$.

A lift can be defined as the force exerted on a body in a direction perpendicular to the direction of flow. There will be the presence of lift if there is a circulatory flow of fluid about the body such as that present about a spinning cylindrical shape [6]. Coefficient of Lift(CL) is a dimensionless coefficient that gives a relationship between generated lift by airfoils, a reference area associated with the body and dynamic pressure of the fluid flow around airfoil [7]. The drag is defined as the force exerted on the body in a direction that is parallel to the direction of flow [6]. Other important parameters are the Drag Coefficient (CD) and the Angle of Attack (AOA). The CD is a dimensionless quantity, utilized in a fluid environment such as air [8], while the Angle of Attack is defined as the angle between the relative wind and chord line as illustrated in Figure 1 below. Mathematical expressions for Coefficient of Lift (CL), Drag coefficient (CD) and Reynolds number (Re) are also shown below (Equations 1, 2 and 3).

quantifying the resistance or drag of an object

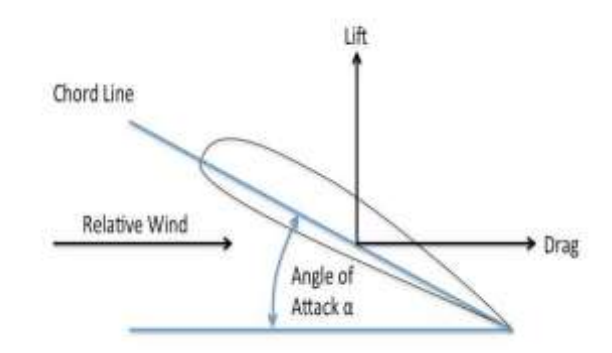


Figure 1: Forces acting on airfoil.

The goal of this work focuses on presenting a description of the physics of flow in response to the enhancement of lift and elimination of drag on airfoils. The investigation of the aerodynamic characteristics of different aerofoil has been studied by researchers. However, there is still dirt of data on a comparative study of the studied characteristics over another. Hence, the need to determine the characteristic of NACA 0008 and 0020 series for design optimization.

$$CL = \frac{FL}{\frac{1}{2}\rho V^2 A} \tag{1}$$

$$CD = \frac{F_D}{\frac{1}{2}\rho V^2 A} \tag{2}$$

$$Re = \frac{\rho V d}{\mu} \tag{3}$$

where:

CL is the lift coefficient CD is the drag coefficient ρ is the density of the fluid F_D is the drag force FL is the lift force A is the area V is the velocity of the object

II. Materials and MethodsA. Airfoil Geometry Generation

NACA 0008 and NACA 0020 are shown in Figures 2a and 2b below as 2 dimensional (2D) sketch respectively. Airfoils coordinates were extracted from airfoiltools.com database, which was then imported into ANSYS Workbench, to generate the 2D airfoil geometry.

B. Mesh Generation of Airfoils

In the analysis of fluid flows, flow domains are divided into smaller subdivisions. Analysis of Mesh was carried out with the assumption that relevance centre is fine and high smoothing in C-mesh domain as shown in Figures 3a and 3b below. Outer sharp corners, like those found on the trailing edge of the airfoil, constitute meshing difficulties. The inside of each subdomain were solved following the discretized method.

C. Boundary Conditions and Input Parameters

Boundary conditions and input parameters are presented in Table 1. These were analyzed for the airfoils at separate angles of attack (0°, 4°, 8°,12°) to determine their aerodynamic characteristics.

Table 1: Table on Boundary Conditions and Input Parameters

No	Input Parameter	Value
1	Type of Fluid	Air
2	Flow Velocity	43m/s
3	Operating Pressure	1 atm
4	Fluid Density	1.225 kgm ⁻³
5	Reynolds Number	10^{6}
6	Length of Chord	1 m
7	Input Temperature	289K
8	Angles of Attack	0°, 4°, 8° and
		12°
9	Realizable Model	Shear stress
		transport
10	Viscosity	$1.009 \times$
		10^{-5}kg/ms

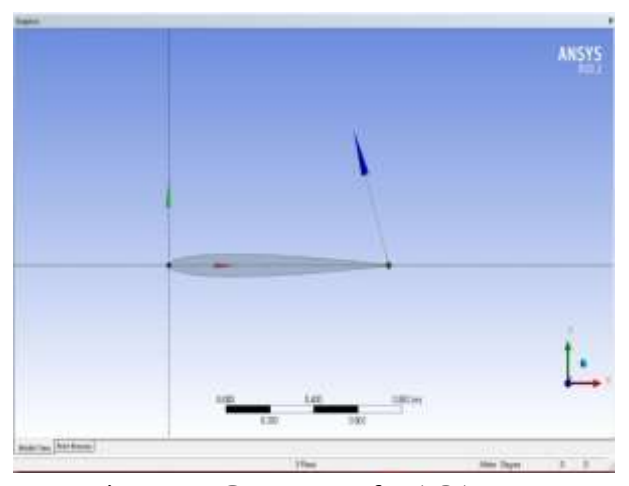


Figure 2a: Geometry of NACA 0008

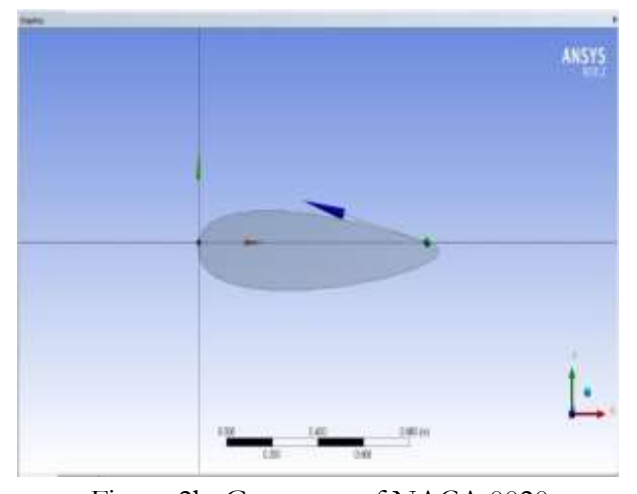


Figure 2b: Geometry of NACA 0020

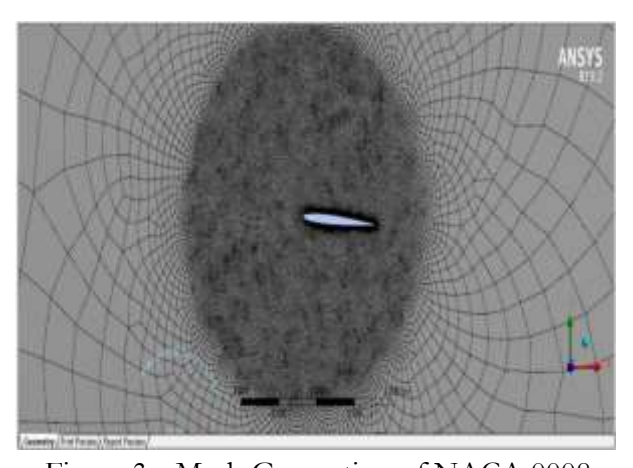


Figure 3a: Mesh Generation of NACA 0008

III. Results and Discussion

A. Magnitude of Contours Velocity

The velocity contours at 0°, 4°, 8° and 12° angles of attack were obtained for NACA 0008 and NACA 0020. The results for the simulations are shown in Figures 4 - 7 below. At 0° angle of attack, it was observed in both NACA 0008 and NACA 0020 at the leading edge that there exists a point of stagnation where the flow velocity is approximately zero for NACA 0020 airfoil with NACA 0008 having a higher concentration of velocity at both lower and upper surface. At a 4° angle of attack, there exists a stagnation point at the leading edge of both airfoils and the velocity flow is seen to have accelerated at the upper surface of both airfoils with NACA 0020 having a more pronounced flow of velocity. At the lower surface, velocity flow is different and lesser, towards the trailing edge, separation can be seen to have occurred in both airfoils. The results obtained are similar to the work carried out by [10].

For 8° and 12° angles of attack, it was observed that the velocity is gradually reduced towards the leading edge and the separation region around the trailing edge increases as well, especially in NACA 0008 which experiences heavy separation

B. Static Pressures Contour

For structural design, estimation of the pressure distribution over an aerofoil is desirable especially when tests are not available. At zero lift the pressure distributions over the upper and lower surfaces are identical. Contours of static pressure show that static pressure increases at the lower surface of the aerofoil with an increasing angle of attack. Figures 8 to 11 show the simulation consequences of static pressure for 0° to 12° AOA for the viscous model of air as a fluid medium. According to the figure underneath at 0° AOA, NACA 0015 has a static pressure

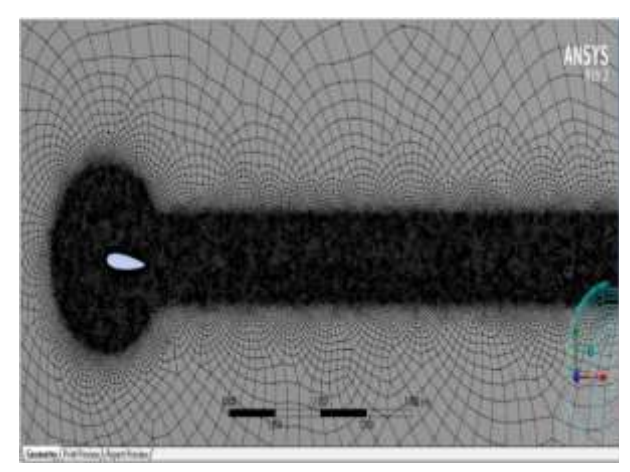


Figure 3b: Mesh Generation of NACA 0020

of 1.160×10^3 which was observed to be greater than 1.113×10^3 Pa as obtained for NACA 0020 aerofoil. That clearly indicated that NACA 0008 will have a greater pressure gradient at small AOA. Hence, for the lift, the pressure on the lower side of the aerofoil is higher than that of the inward flow stream and effectively pushed the aerofoil upward. Static pressure increases to a maximum of 1.192×10^3 Pa for NACA 0008 more than 1.114×10^3 Pa for NACA 0020 aerofoil, at 4° AOA with a quiet laminar flow pattern. Also at other angles of attack, NACA 0008 seems to have more static pressure distribution than NACA 0020 aerofoil.

Generally, at high pressure regions, it was observed that velocity of flow was a bit restricted (lower surface of the airfoil) and where pressure was low, a higher flow of velocity was observed. This behaviour is similar to that reported by [10]

C. Drag and Lift Curve

Figure 12 presents the drag, lift as well as their coefficients for NACA 0008 at each angle of attack. The results obtained show that the lift coefficient increases as the angle of attack increases. This is due to the propagation of flow separation points up to the leading edge as the angle of attack increases.

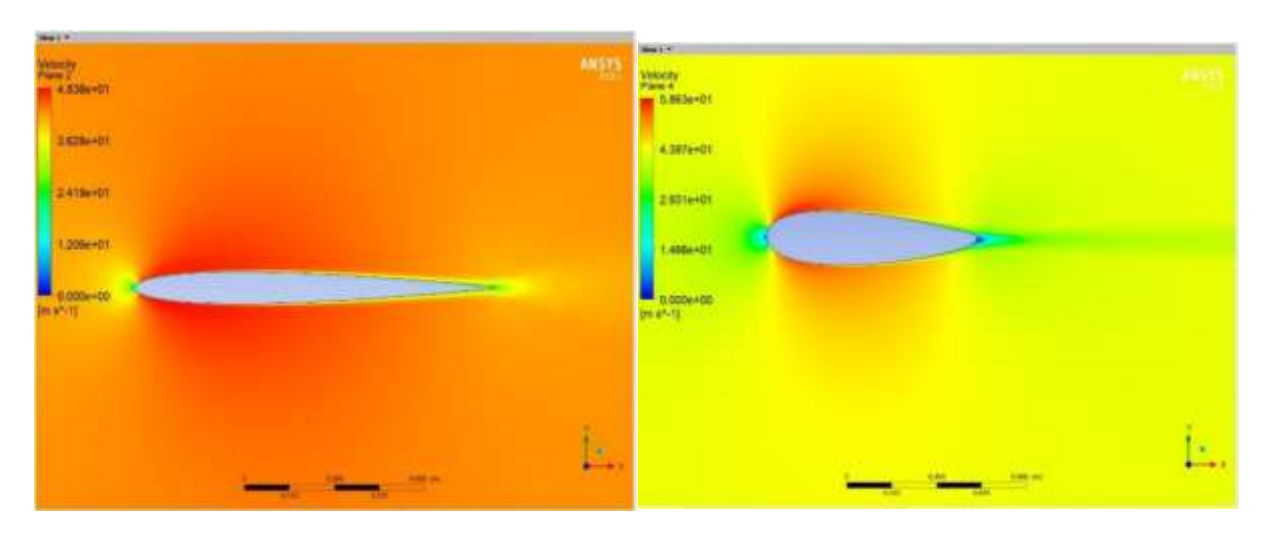


Figure 4: Velocity contours of NACA 0008 and NACA 0020 at 0° angle of attack

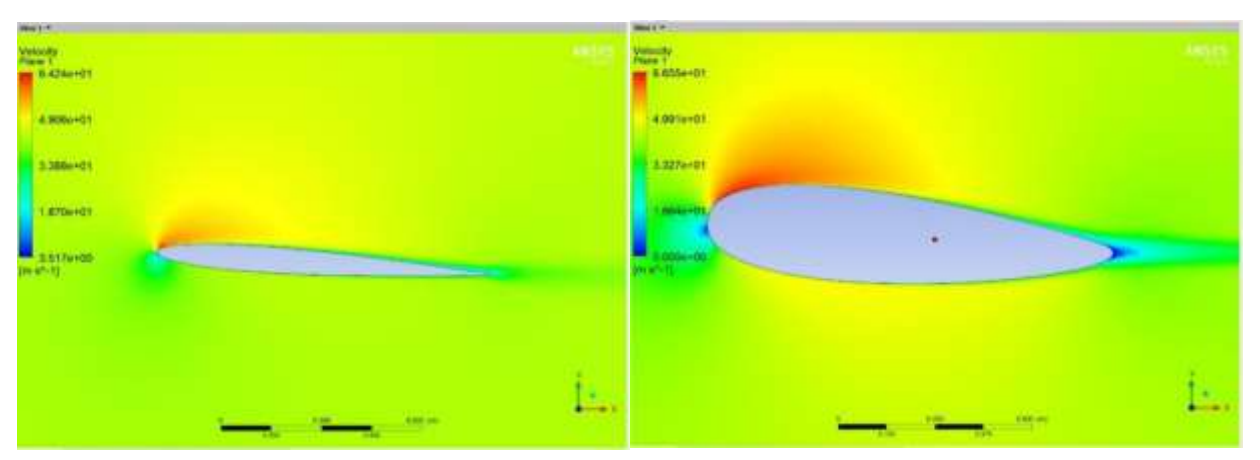


Figure 5: Velocity contours of NACA 0008 and NACA 0020 at 4° angle of attack

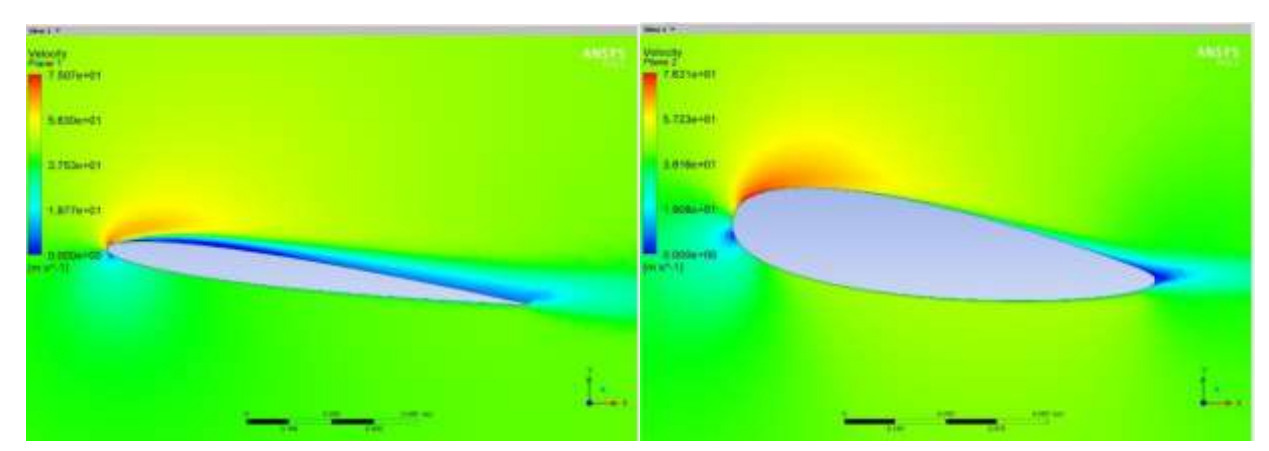


Figure 6: Contours velocity of NACA 0008 and NACA 0020 at 8° angle of attack

.

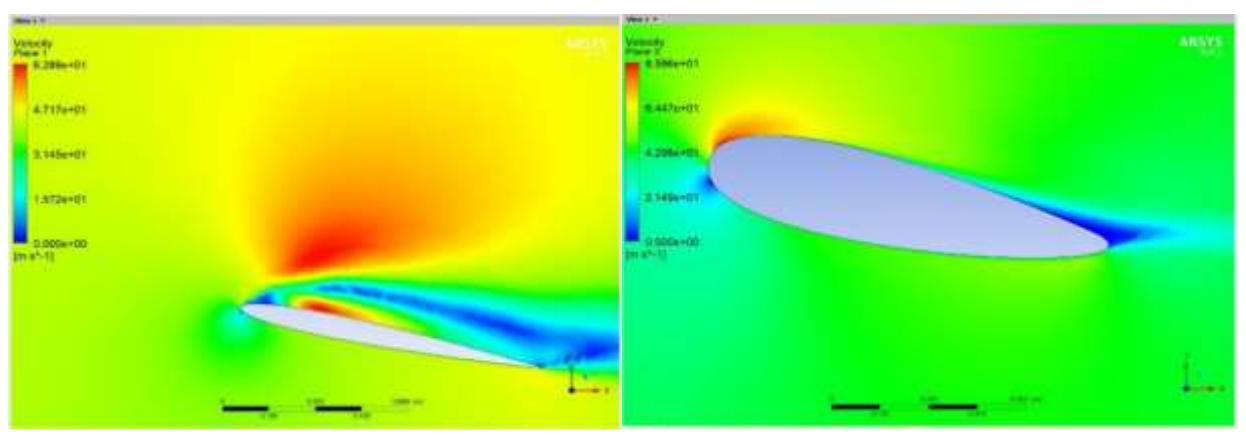


Figure 7: Contours velocity of NACA 0008 and NACA 0020 at 12° angle of attack

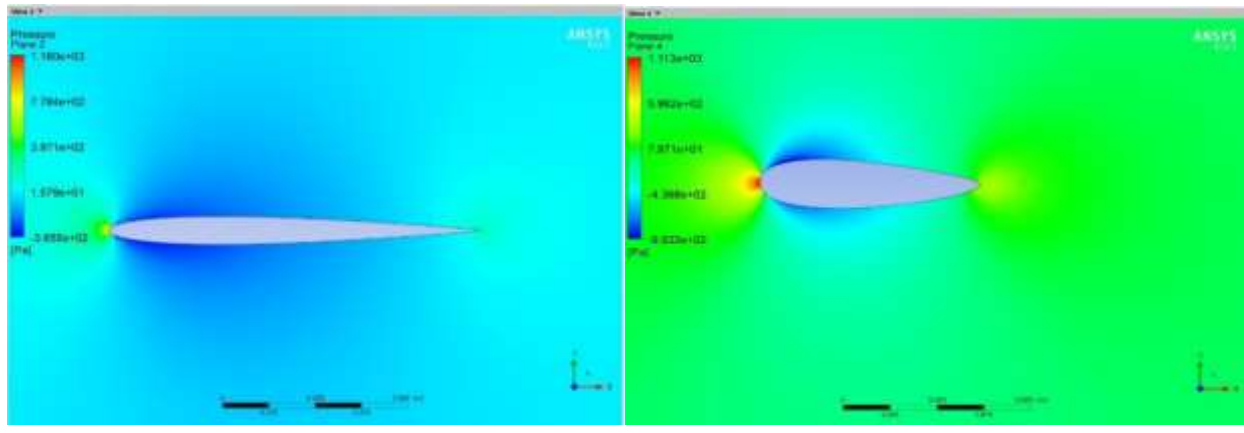


Figure 8: Pressure contours of NACA 0008 and NACA 0020 at 0° angle of attack

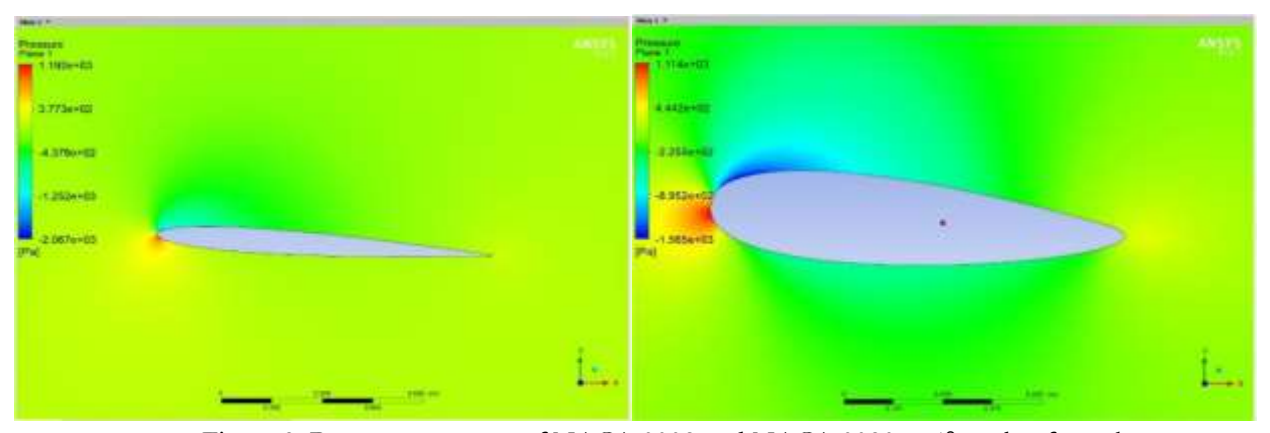


Figure 9: Pressure contours of NACA 0008 and NACA 0020 at 4° angle of attack

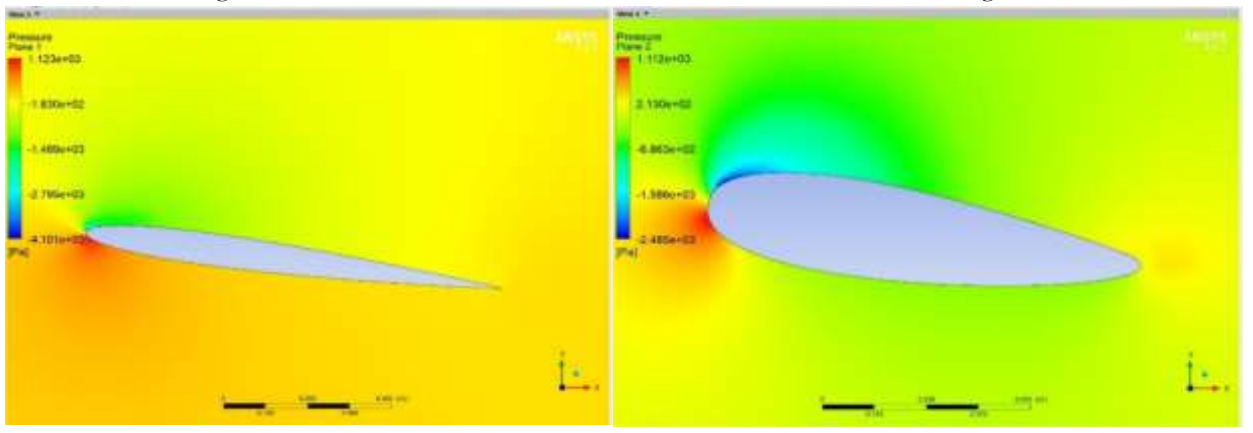


Figure 10: Pressure contours of NACA 0008 and NACA 0020 at 8° angle of attack

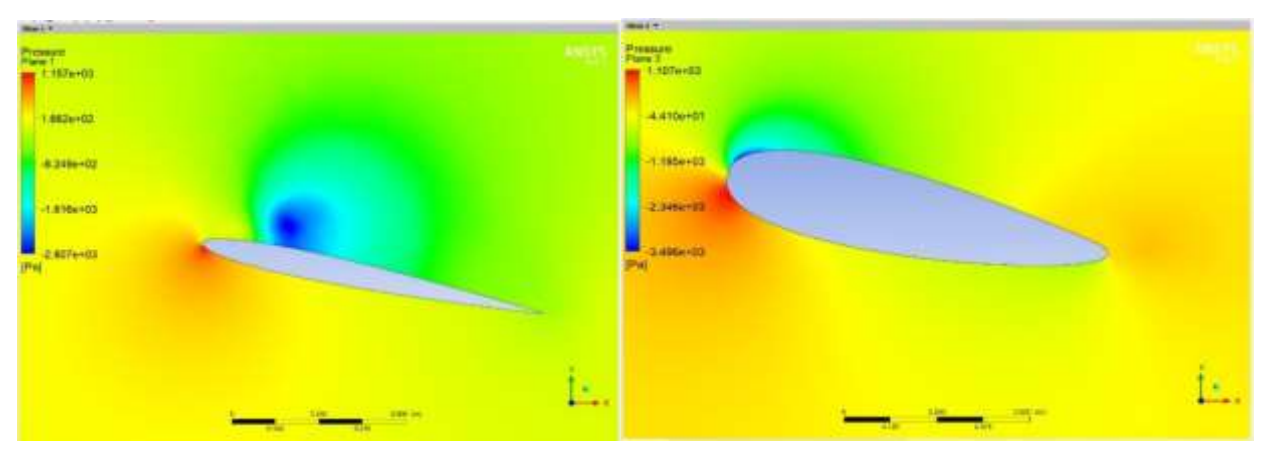


Figure 11: Pressure contours of NACA 0008 and NACA 0020 at 12° angle of attack

.The effect of angle of attack (AOA) on the drag coefficient also shows that as the angle of attack increases the drag coefficient also increases. This is as a result of an increase in pressure distribution values over the lower surface of the airfoil. The obtained results is in close agreement with that obtained by [11] who performed a comparative study on NACA0012, NACA2412, and SG6043 at different AOA.

Similarly, Figure 13 describes the drag, lift as well as their coefficients for NACA 0020 at each angle of attack. The obtained results reveal that the lift coefficient increases as the angle of attack also increases. This is equally a result of the propagation of flow separation point up to the leading edge as the angle of attack increases. The effect of angle of attack (AOA) on the drag coefficient also revealed that as the angle of attack increases there is an increase in the drag coefficient.

This is due to pressure distribution values increasing over the lower surface of the airfoil. This is as reported by [11] who performed a comparative study Figure 14 illustrates the lift to drag ratio of NACA 0008 and 0020 respectively. The lift to drag ratio generally increases with increasing AOA. For NACA 0008 and 0020, lift to drag ratio increases up to 8° angle of attack after which it starts decreasing. NACA 0008 was observed to have

the highest value for lift to drag ratio which can be applied in wind turbine applications.

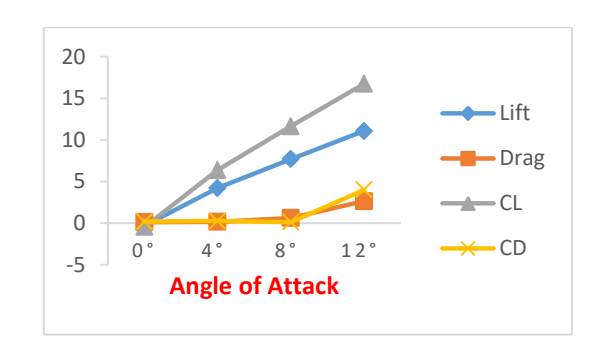


Figure 12: Relationship between lift, drag and their coefficients on different angle of attach for NACA 0008

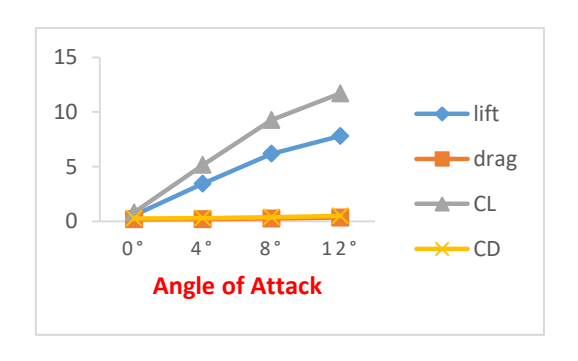


Figure 13: Relationship between lift, drag and there coefficients on different angle of attack for NACA 0020

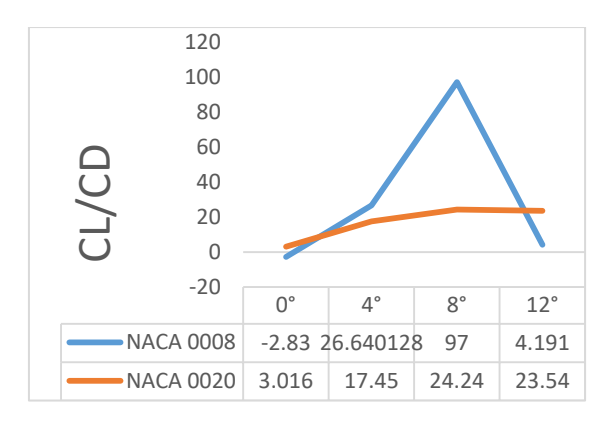


Figure 14: Relationship between lift and drag coefficients ratio against NACA 0008 and NACA 0020

IV. Conclusion

The results from the simulation show that both NACA 0008 and NACA 0020 can be effective at different angles of attack. In each angle of attack, there was an increase in lift and a considerable low increase in drag for both airfoils. However, it was observed that NACA 0008 experienced higher lift at each angle of attack than NACA 0020, except at 0° angle of attack where NACA 0020 had a fraction of lift over the other. NACA 0008 appears to be the best amongst the two airfoils having a greater lift at each angle of attack. Hence, its use in the aerospace industries on NACA0012, NACA2412, and SG6043 at various AOA.

References

- [1] Chandrala, M. "Aerodynamic Analysis of Horizontal Axis Wind Turbine Blade", International Journal of Engineering Research and Applications; (IJERA) ISSN: 2248-9622, vol. 2, no. 6, 2012, pp.1244-1248.
- [2] Hossain, S. "A Comparative Flow Analysis of Naca 6409 and Naca 4412 Aerofoil", IJRET: *International Journal of Research in Engineering and Technology*; eISSN: 2319-1163 pISSN: vol. 3, no. 10, 2014, pp. 2321-7308.

- [3] Patil, S. "Computational Fluid Dynamics Analysis of Wind Turbine Blade at Various Angles of Attack and Different Reynolds Number", *International Conference on Computational Heat and Mass Transfer, Procesia Engineering*; vol. 127, 2015, pp.1363-1369.
- [4] Rubel, R.I., Uddin, M.K., Islam, M.Z. and Rokunuzzaman, M. "Comparison of Aerodynamics Characteristics of NACA 0015 & NACA 4415". Preprints 2016.
- [5] Najar, A. "Blade Design and Performance Analysis of Wind Turbine", *International Journal of ChemTech Research CODEN*; IJCRGG ISSN: 0974-4290, vol.5, no.2, 2013, pp. 1054-1061.
- [6] Burton, T., Jenkins, N., Sharpe, D. and Bossanyi, E. "Wind Energy Handbook", Chichester, UK: *John Wiley & Sons*; 2011, pp. 65-67.
- [7] Şahin, İ. and Acir, A. "Numerical and Experimental Investigations of Lift and Drag Performances of NACA 0015 Wind Turbine Airfoil", *International Journal of Materials, Mechanics and Manufacturing*; vol. 3, no. 1. 2015.
- [8] Coles, D. and Alan, J. "Flying-Hotwire Study of Flow Past an NACA 4412 Airfoil at Maximum Lift", *American Institute of Aeronautics and Astronautics Journal*, vol. 17, no. 4, 1979, pp. 321-329.
- [9] Alley, R.N., Warren, F.P. and Spall, R. "Predicting Maximum Lift Coefficient for Twisted Wings Using Computational Fluid Dynamics", *Journal of Aircraft*; 2007, pp. 890-898.
- [10] Shiming, Xiao and Zutai, Chen. "Investigation of Flow over the Airfoil NACA 0010-35 with Various Angle of Attack", *MATEC Web of Conferences*, 2018, 179, 03020.
- [11] Mohamed, A. "A Comparative Study for Different Shapes of Airfoils", *International*

Journal of Mechanical Engineering, vol. 4, 2019, pp. 27-36.